ELSEVIER

Journal of Alloys and Compounds 300–301 (2000) 322–328

Journal of ALLOYS AND COMPOUNDS

www.elsevier.com/locate/jallcom

Growth and characterization of lithium tantalate single crystals doped with Ho, Tm, Nd, Yb, Pr and doped by diffusion with Cr and Cu

S.M. Kaczmarek[a,*], M. Świrkowicz[b], R. Jabłoński[b], T. Łukasiewicz[b], M. Kwaśny[a]

[a]*Institute of Optoelectronics, MUT, 2 Kaliski Str., 01-489 Warsaw, Poland*
[b]*Institute of Electronic Materials Technology, 133 Wólczyńska Str., 01-919 Warsaw, Poland*

Abstract

Crystal growth conditions for lithium tantalate single crystals doped with rare-earth and conditions of the diffusion process for doping with Cr and Cu are described. Absorption and an additional absorption after γ-irradiation and annealing treatments at room temperature were measured. The γ-irradiation with a dose of 10^5 Gy and subsequent annealing at 800°C in air for 3 h lead to a valency change of Ho and Pr ions. In the case of γ-irradiation a recombination process due to the Compton effect seems to be responsible for the valency change process in both crystals. Luminescence and radioluminescence measurements in UV+VIS range were also performed which show a weak excitation energy transfer from the $LiTaO_3$ lattice to impurity ions. ESR investigations were performed which suggest probable localization of impurities incorporated by diffusion at Li^+ sites, impurities incorporated during growth at Ta^{5+} or interstitial sites and also strong structure deviations in Nd, Yb:$LiTaO_3$ as compared to $LiNbO_3$ single crystals. All single crystals under tests reveal good optical quality and higher absorption than in the case of yttrium–aluminate garnets and lithium niobate with similar level of rare-earth concentration.

Keywords: Ferroelectrics; Crystal growth; Optical properties; Point defects; Electron paramagnetic resonance

1. Introduction

Lithium tantalate is one of the promising materials for planar wave-guide lasers for optical telecommunication. Solid state, resistant materials emitting in an appropriate wavelength region (1.5 μm) with high efficiency, and cheap to produce, are needed. Ferroelectric materials are interesting due to the possibility of applying the lasing effect and also non-linear effects in the same specimen. One of the candidates is $LiTaO_3$ which has a Curie point at ca. 610°C and trigonal structure and is used widely as a surface acoustic wave substrate, electro-optic modulator and second harmonic generation material [1]. Recently, there have been successful attempts at using Nd:$LiTaO_3$ for construction of a wave-guide laser [2] and also a diode-pumped (800 nm) 'slab' type laser. For both polarizations, σ and π, output energy of about 10 mW was obtained for pump power of about 70 mW [3].

The main purpose of this work was to determine the conditions of single crystal growth by the Czochralski method of lithium tantalate doped with rare-earths and the measurement of optical properties and ESR spectra of the crystals obtained. Conditions of thermo-diffusion (temperature, period) for $LiTaO_3$ crystals doped with transition metal ions, Cr and Cu, were also found.

2. Experimental procedure

2.1. Crystal growth

The main problem during $LiTaO_3$ growth is determining the charge composition which leads to axially uniform single crystals [4–7]. According to Curie temperature measurement in this work it has been found that the best results may be obtained for the following composition:

48.75 mol.% Li_2O:51.25 mol.% Ta_2O_5. (1)

All the growth charges were prepared according to this formula starting from Li_2CO_3 of 4N-purity, from the Institute of Electronic Materials Technology, Warsaw, and Ta_2O_5 of 4.5N-purity made in China. Mixed materials were put into a Pt container and then heated at 1250°C for

*Corresponding author.

0925-8388/00/$ – see front matter
PII: S0925-8388(99)00732-X

6 h. Such solid state reaction gives only the $LiTaO_3$ phase which was confirmed by X-ray analysis. Dopants (rare-earth oxides) were added to the charge.

For crystal growth, an iridium crucible, 50-mm in diameter and height, was used. Two different thermal systems – one with active and the other with passive iridium afterheater were prepared and temperature profiles were measured. Axial temperature distributions were measured with use of a Pt6%Rh–Pt30%Rh thermocouple and MTB-2k meter made by Thermolab (Poland). According to these measurements an axial temperature gradient near the melt surface is equal to 100 K/cm for the passive afterheater but about 50 K/cm for the active one. The two thermal systems give the possibility of adjusting the growth conditions to potential needs.

All melting and crystal growth runs were performed using an r.f. heated Czochralski apparatus (MSR-2 made by Metals Research Ltd., UK) equipped in a computer regulated automatic diameter control unit with a Sartorius electronic balance. The following elements and concentrations were used: Pr (0.05 at.% and 0.5 at.%), Nd (0.5 at.%), and Yb (0.7 at.%), Tm (0.43 at.% and 0.72 at.%) and Ho (0.3 at.% and 0.5 at.%).

At the beginning undoped single crystals were grown. The conditions were the following: pulling rate, 4 mm/h; rotation rate, 18–20 rev./min; active afterheater, nitrogen flow 200 ml/min and, cooling after growth 24 h. Colorless single crystals 18 mm in diameter and 50 mm in length were obtained. Depending on the dopant, the pulling rate changed from 0.8 mm/h for thulium to 2 mm/h for praseodymium and the rotation rate was in the range of 10 to 30 rev./min. After removing crystals from the melt they were cooled down to room temperature for 24 h. In the case of Pr^{3+} doping, a thermal system with active afterheater was used. For other dopants a passive afterheater in different positions with respect to the r.f. coil turned out to be suitable.

Diffusion of Cr and Cu was performed in Cr_2O_3 and CuO, respectively. The temperature was changed from 750 to 1100°C. All annealing treatments were done in air.

2.2. Optical measurements

The samples for optical measurements cut out perpendicularly to either *Z* or *Y* directions were polished on both sides to a thickness of about 1 mm. The samples were irradiated by gamma photons immediately after the crystal growth process. A gamma source of ^{60}Co with a strength of 1.5 Gy/s was used. The gamma doses applied were up to 10^6 Gy.

Optical transmission was measured before and after γ-irradiation and/or annealing treatments using a LAMBDA-2 Perkin-Elmer spectrophotometer in the UV–VIS range and FTIR-1725 in the IR range. According to the measured transmission the absorption was calculated. Additional absorption was calculated according to the formula:

$$\Delta K(\lambda) = (1/d)\ln(T_1/T_2) \quad (2)$$

where K is the absorption, λ is the wavelength, d is the sample thickness and T_1 and T_2 are transmissions of the sample before and after a treatment, respectively.

Fluorescence spectra were obtained in the range 200 to 800 nm using a Perkin-Elmer spectrofluorimeter LS-5B. Excitation with lasers of wavelength 355, 442 and 530 nm was also applied.

Radioluminescence spectra were obtained in the range 200 to 850 nm using X-ray excitation (DRON, 35 kV/25 mA) and an ARC Spectra Pro-500i spectrograph: ARC Spectra Pro-500i (diffraction grating Hol-UV 1200 gr/mm and diffraction grating brighten up at 500 nm 1200 gr/mm, 0.5 mm slits), PMT: Hamamatsu R928 (1000 V).

2.3. ESR measurements

The dimensions of samples for ESR investigations were 3.5×3.5×2 mm. They were investigated in a Bruker ESP300 ESR spectrometer (X-band). The spectrometer was equipped with a helium flow cryostat type ESR900 from Oxford Instruments. The ESR investigations were performed in the temperature range from 4 to 35 K and microwave power from 0.002 to 200 mW.

3. Results and discussion

3.1. Absorption and additional absorption

The level of crystal imperfection can be in first approximation estimated by the absorption and especially by additional absorption measurements after irradiation with e.g. γ-quanta and thermal annealing in an appropriate atmosphere. It is involved in the absorption value (optical density of a crystal) and additional absorption bands (their shape and position which suggest color centers appearing due to particular treatment).

The fundamental absorption edge in the case of Cr doping by diffusion is equal to 267 nm, so it is the same as for undoped material and is independent of dopant concentration. In the case of crystals doped during growth the absorption edge shifts to about 275 nm except for the Pr (0.5 at.%):LT crystal when it is equal to 320 nm. In Cu-doped LT crystals FAE changes with Cu concentration. It should be emphasized that absorption caused by rare-earth ions is higher for LT single crystals than for yttrium–aluminum garnet (YAG) with the same doping level.

In the absorption spectrum of LT single crystals doped during growth there arise very clear bands due to an existence of OH^- ions in the lattice (2871 nm band). It suggests that rare-earth ions are located in the LT lattice in other positions than Li^+ sites. In the case of doping by

diffusion with Cr or Cu only weak absorption is observed near the wavelength corresponding to the OH^- line. These observations suggest that location of active ions depends on the method of doping. In the case of doping by thermo-diffusion a decrease of intensity of OH^- absorption bands leads to the conclusion that ion dopants are introduced into Li^+ sites in the LT lattice. On the other hand, doping during growth probably leads to an incorporation of active ions into Ta^{5+} sites or interstitial positions with octahedral symmetry. Incorporation of dopants into Li^+ sites during thermo-diffusion can be explained in the following way. It is evident that in LT single crystals obtained from the congruently melting composition the principal defects are lithium vacancies. During the diffusion process at elevated temperatures dopant ions occupy these vacancies. For crystals doped during growth other positions in the LT lattice (e.g. Ta^{5+}) are energetically more favorable. The OH^- absorption band in diffusely doped LT single crystals is broader than in crystals doped during growth which suggests that they have more defects.

For LT crystals doped by diffusion, absorption curves show that the factors limiting the diffusion process are temperature and period. At lower temperatures than 900°C the diffusion process is slower, moreover, in a shorter period the amount of impurity entering the crystal is lower and the crystal shows a higher imperfection.

After γ-irradiation of LT single crystals doped with rare-earth, independently of the dopant, additional absorption bands appear with maxima at wavelengths: 311, 394, 2871 and 4200 nm. In the first band region the crystal is brightened up, the second is connected with some color center, the third is due to a change in OH^- concentration and the fourth could be connected with f–f transitions. Observations of changes in absorption of diffusely doped crystals suggest that an intensity of the first band is in some way related to the imperfection connected with the doping process.

An increase of praseodymium content leads to an improvement of LT lattice structure and additional absorption decreases. A similar effect has been observed for yttrium aluminum perovskite (YAP) single crystals doped with praseodymium [8]. As was confirmed by Curie temperature measurements for samples cut from the origin and end of the crystal (changes about ±2 K in a value of Curie temperature at an accuracy of measurement ±1 K), the crystals showed uniform longitudinal impurity distribution. Also X-ray probe measurements show uniform praseodymium distribution. On the basis of these measurements one can say that the Pr segregation coefficient in the LT crystal is nearly 1.

The highest amount of point defects exist in Nd, Yb:LT crystals; there is a deep minimum at 311 nm and a large additional absorption at 394 nm. Doping with Tm and Ho leads to similar results in additional absorption, with the exception of characteristic bands for Ho:LT crystals, caused by transitions in Ho^{3+}. Perhaps, it is a result of a valency change of Ho^{3+} ions due to γ-quanta irradiation; probably Ho^{3+} ions capture Compton electrons and become divalent. The change in valency of Ho ions is clearly seen also in Fig. 1g and h where an additional absorption after γ-irradiation is depicted with an additional absorption after annealing the irradiated crystals at 800°C in air for

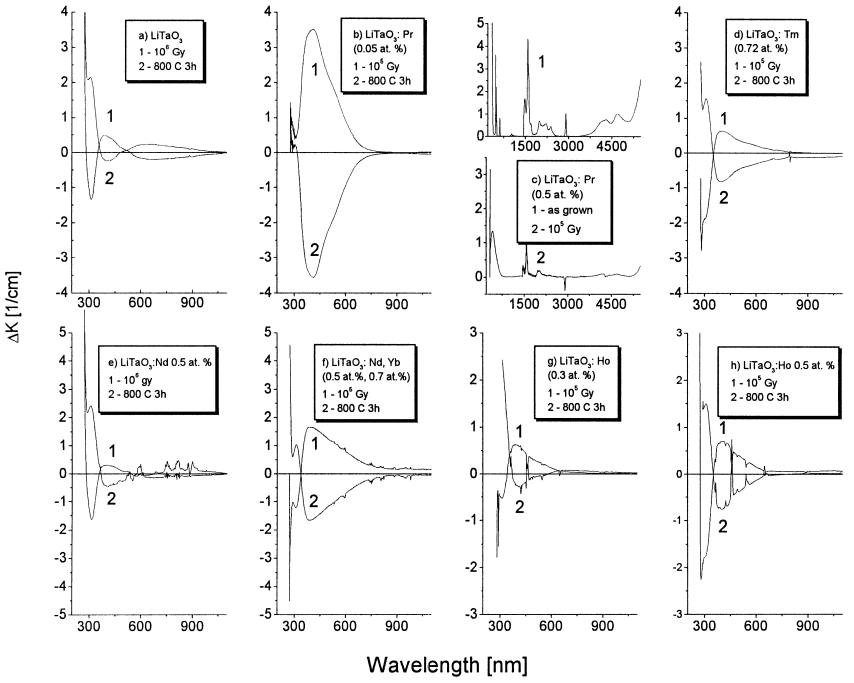

Fig. 1. An additional absorption of lithium tantalate single crystals after successive irradiation and annealing at 800°C in air for 3 h.

3 h. The annealing leads to a valency change of Ho ions in the opposite direction ($Ho^{2+} \rightarrow Ho^{3+}$).

Similarly as in Ho:LT, Pr:LT single crystals also show valency changes of Pr ions after γ-irradiation. In this case, in the IR range of the absorption spectrum an additional absorption characteristic for intra-atomic transitions in Pr is observed (Fig. 1c). An effect of the capture of Compton electrons by Pr^{4+} ions is that they become trivalent. According to Fig. 1c, a valency change of Pr ions is accompanied by a decrease in OH^- concentration (2871 nm band) and depends on the Pr starting concentration. Moreover, valency changes of Ho and Pr ions are accompanied by additional absorption after γ-irradiation which is observed in the far infrared part of the absorption spectrum (a band close to 4200 nm).

According to Fig. 1 an annealing at 800°C for 3 h in air almost completely removes an additional absorption caused by γ-irradiation in doped-during-growth LT single crystals.

In Fig. 2, absorption and additional absorption after γ-irradiation with a dose of 10^5 Gy for undoped and Cr, Tm, Nd, Nd+Yb, Ho and Pr doped LT single crystals in the wavelength range 2500 to 4500 nm are presented. The absorption changes in diffusely doped crystals suggest that dopant ions are incorporated into Li^+ sites in the LT lattice. The conclusion is confirmed by Fig. 2a, where a decrease in absorption at the wavelength is observed after γ-irradiation for crystals diffusely doped with Cr. According to Fig 2c, f and h, Tm and Ho ions are located in different lattice sites than Li^+ sites. It seems to be dependent on the dopant concentration too (see Fig. 2g, h for Ho and Fig. 2i, j for Pr).

As compared with lithium niobate, an additional absorption of LT single crystals (0.45 cm^{-1} for 394 nm band) is similar in value and shape and its lower value for Cr crystals doping by diffusion suggest that chromium can be introduced into lithium tantalate easier than to lithium niobate. Probably, the 394 nm band corresponds to a 385 nm band for lithium niobate, which is caused by F centers [9]. The 311 nm band has no equivalent band in the lithium niobate absorption spectrum but a similar kind of brightening is observed for LN crystals near 350 nm [10].

We suspect that a negative change of the 2871 nm band after γ-irradiation indicates a change in imperfection of the LT crystal, and may be an increase in concentration of dopant ions placed at Li^+ sites. Positive change of the 2871 nm band after γ-irradiation may indicate a decrease in concentration of dopants located at Li^+ sites. So, γ-irradiation significantly changes imperfection of the LT single crystal.

3.2. Radioluminescence and luminescence measurements

In Fig. 3 luminescence (a–d) of LT single crystals doped with: (a) Ho (0.5 at.%), (b) Nd (0.5 at.%), (c) Tm (0.72

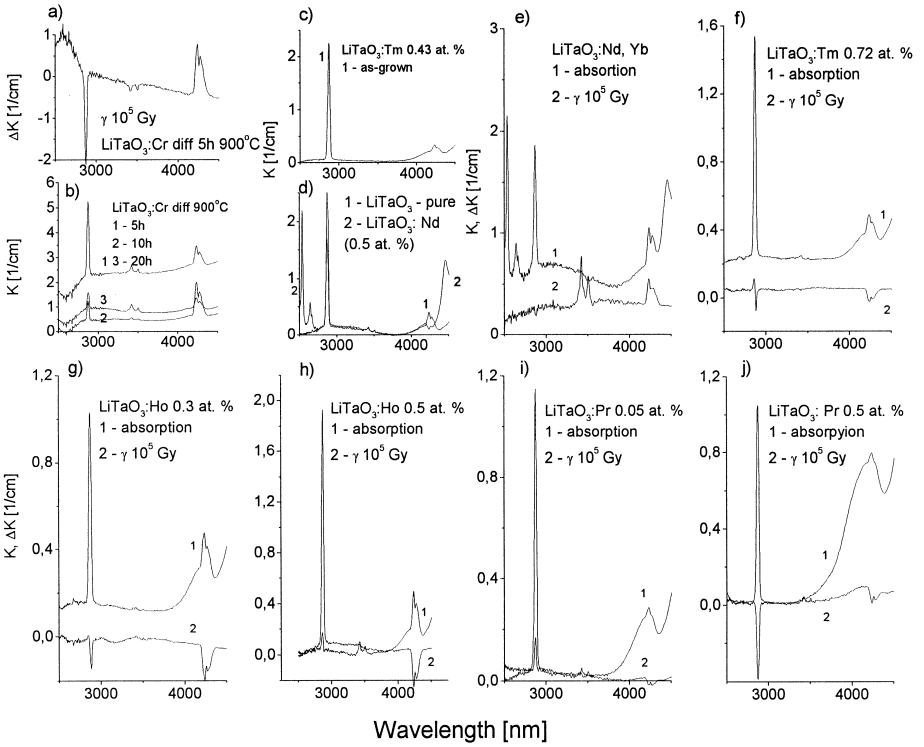

Fig. 2. The absorption and additional absorption of LT single crystals in the near infrared region: (a and b) crystals diffusely doped with Cr; (c) Tm (0.43 at.%):LT; (d) undoped (curve 1), Nd (0.5 at.%):LT (curve 2); (e) Nd and Yb:LT; (f) Tm (0.72 at.%):LT; (g) Ho (0.3 at.%):LT; (h) Ho (0.5 at.%):LT; (i) Pr (0.05 at.%):LT and (j) Pr (0.5 at.%):LT.

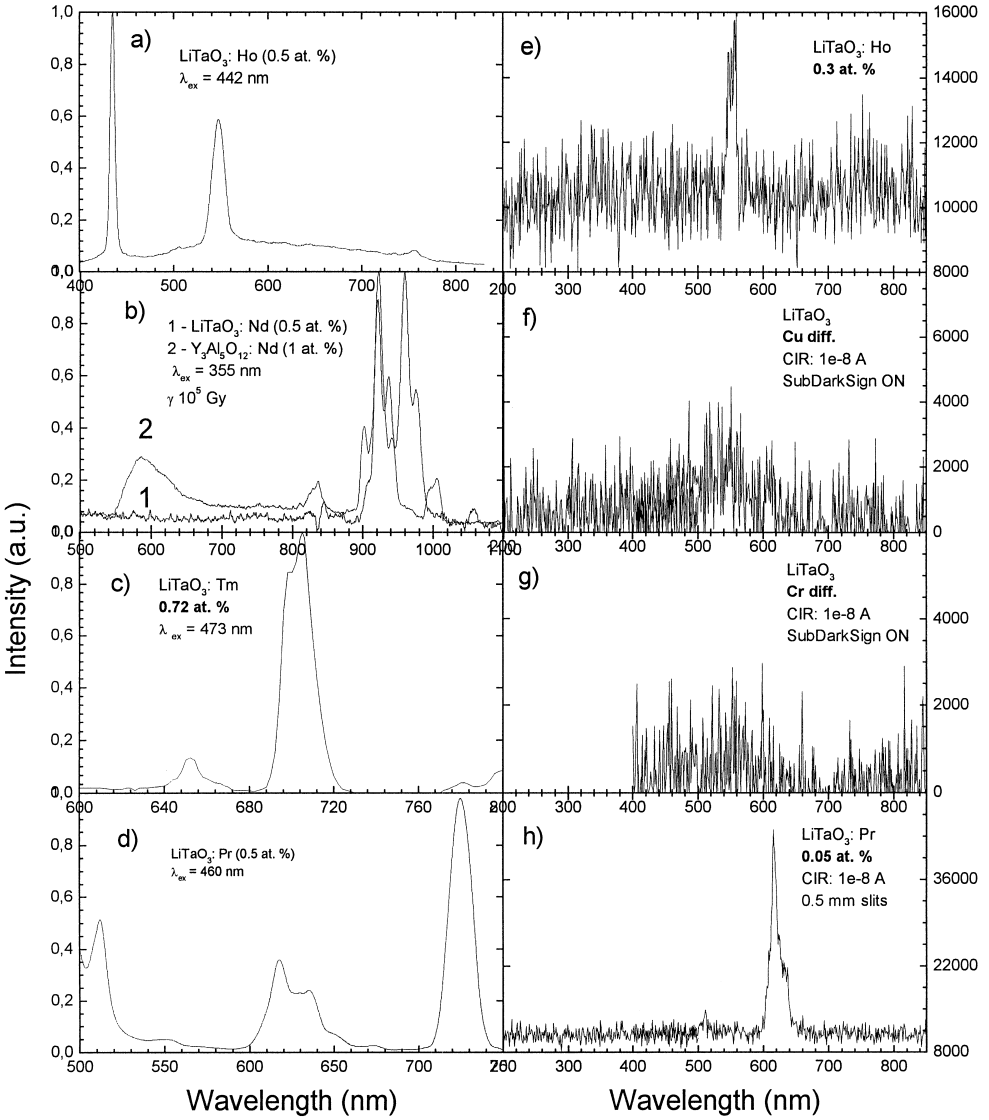

Fig. 3. (a–d) Uncorrected luminescence spectra of Ho (0.5 at.%):LT, Nd (0.5 at.%):LT, Tm (0.72 at.%):LT and Pr (0.5 at.%):LT, respectively and (e–h) radioluminescence spectra of Ho (0.3 at.%):LT, Cu(dif.):LT, Cr(dif.):LT and Pr (0.05 at.%), respectively.

at.%) and (d) Pr (0.5 at.%) and radioluminescence (e–h) of diffusely doped LT crystals with (f) Cu and (g) Cr and doped during growth (e) Ho (0.3 at.%) and (h) Pr (0.05 at.%) measurements are presented. Among crystals doped during growth, clear luminescence bands show: in the VIS range – Ho:LT (550 and 760 nm bands), Tm:LT (652 and 705 nm bands), Pr:LT (515, 620 and 720 nm bands) and Nd (1 μm) in the IR range. The crystals doped diffusely show a weak luminescence and do not show any radioluminescence bands. Among all crystals under test only Ho:LT (550 nm band) and Pr:LT (620 nm band) reveal a clear radioluminescence spectrum. It may indicate that in LT single crystals excitation energy transfer from lattice to impurity ions is rather weak.

3.3. Electron spin resonance

ESR spectra were measured for all crystals under test. Moreover, ESR spectra for powdered Nd:LT and Nd, Yb:LT single crystals were done. In Fig. 4a and b, polycrystalline spectra of Nd:LT and Nd, Yb:LT crystals are depicted. They are presented due to a problem in separating Nd and Yb ESR lines in Nd, Yb:LT single crystals. As seen from Fig. 4c–e the ESR spectrum of Nd, Yb:LT single crystal is, unfortunately, isotropic. We suspect that Nd, Yb:LT single crystal has a lot of defects due to e.g. competition of Nd and Yb ions in substituting lattice sites. Such a conclusion is confirmed by absorption spectra measurements of Nd- and Yb-doped LN and LT

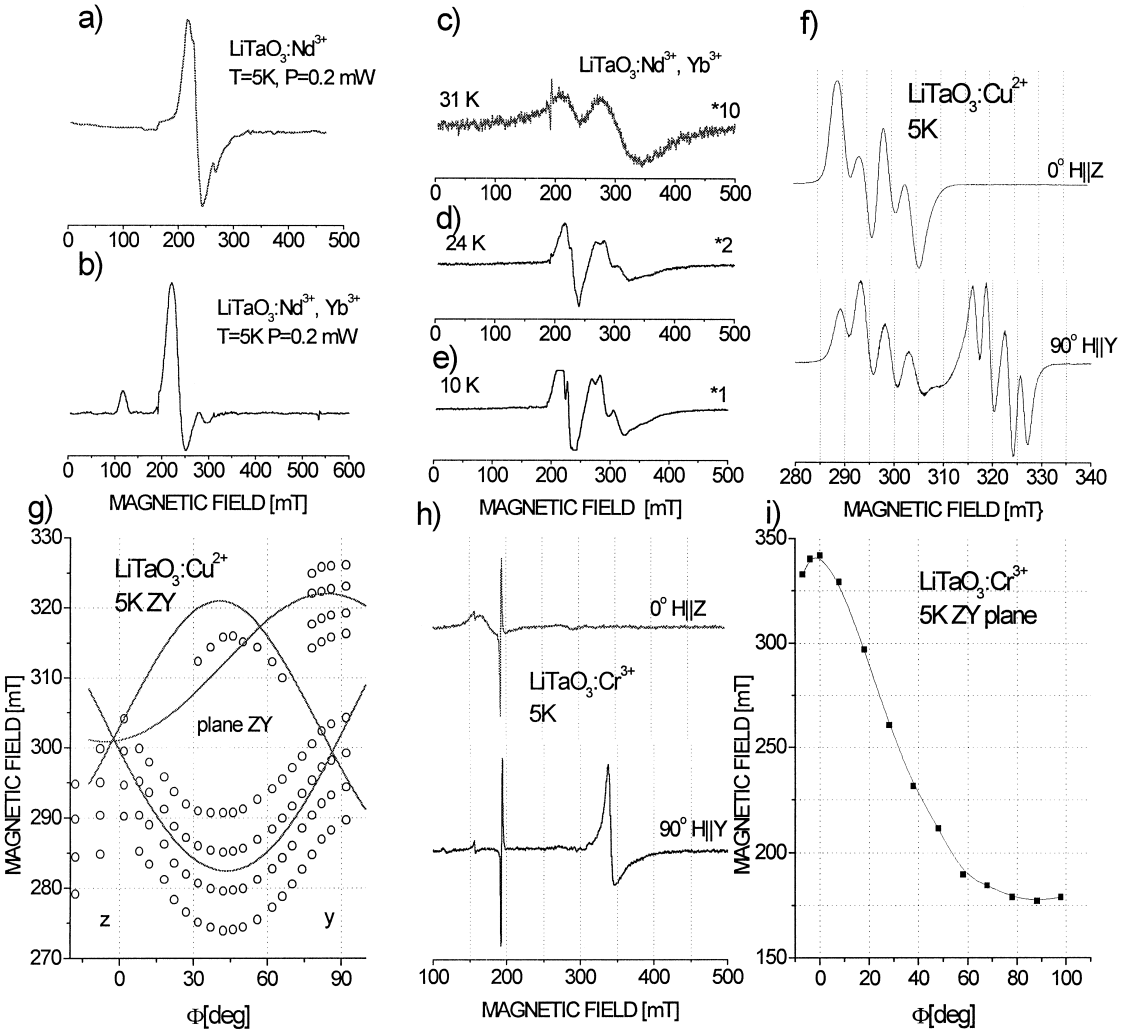

Fig. 4. Derivative ESR spectrum of polycrystalline (a) Nd:LT and (b) Nd, Yb:LT, ESR spectrum of single crystal Nd, Yb:LT for (c) 31 K, (d) 24 K and (e) 10 K, (f–i) ESR spectra of crystals doped by diffusion: (f) Cu:LT for $H\|Z$ and $H\|Y$, (g) angular dependence for Cu:LT – circles, experiment and solid lines, calculated values for the centers of hyperfine lines, (h) Cr:LT for $H\|Z$ and $H\|Y$ and (i) angular dependence for Cr:LT in ZY plane.

single crystals. In the first case strong absorption of Yb with respect to Nd ions is observed in the absorption spectrum, while in the second case this absorption is a weak one.

Fig. 4f–i shows ESR spectra for diffusely doped (f and g) Cu:LT and (h and i) Cr:LT crystals. The lines presented in this figure are anisotropic and measured for the following angles: 0° ($H\|Z$) and 90° ($H\|Y$). Their angle dependences are depicted in (g) and (i) for Cu:LT and Cr:LT, respectively. As seen, for Cu:LT crystals we are dealing with four characteristics for Cu^{2+} ion lines of hyperfine structure ($I = 3/2$). For the effective electron spin Hamiltonian one can write:

$$\boldsymbol{H} = \beta \cdot g \cdot H \cdot S + A \cdot I \cdot S \quad (3)$$

where: $S = 1/2$, $H_{\mathrm{res}} = \nu/(g\beta/h)$, β is the Bohr magneton, θ is the angle between the magnetic field and the z-axis, h is the Planck constant, g is the Lange factor, ν is the microwave frequency, H_{res} is the resonance magnetic field and:

$$g^2 = g_x^2 l^2 + g_y^2 m^2 + g_z^2 n^2$$

with l, m, n direction cosines, I the nucleus spin, and A the hyperfine structure constant.

The values of hyperfine A constant ($A \times 10^{-4}$ cm^{-1}) and g_x, g_y and g_z, calculated in this paper, were compared with literature data on $LiNbO_3$:Cu^{2+} in Table 1.

Angle dependences for diffusely doped with Cr lithium tantalate crystal (Fig. 4i) show a single line, which can be described using the following electron spin Hamiltonian:

$$H = g \cdot \beta \cdot \boldsymbol{H} \cdot S \quad (4)$$

Table 1
Hyperfine A constants ($\times 10^{-4}$ cm^{-1}) and Lande factor values for Cu^{2+}:LT as compared to Cu^{2+}:LN crystal [11]

$LiNbO_3$:Cu^{2+} [11]		$LiTaO_3$:Cu^{2+}	
$g_x = 2.076(5)$	$A_x = 50.5(1)$	$g_x = 2.08(2)$	$A_x = 32.15(5)$
$g_y = 2.106(5)$	$A_y = 30.2(1)$	$g_y = 2.10(2)$	$A_y = 65.5(2)$
$g_z = 2.381(5)$	$A_z = 78.0(1)$	$g_z = 2.43(5)$	–

where $S = 1/2$. Calculated values of the Lande factor are as follows: $g_{\|} = 1.9660$ and $g_{\perp} = 3.7595$.

From the above angle dependences, it results that Cu^{2+} or Cr^{3+} ions do not substitute Li^+ sites only. Kobayashi et al. [11] suggest that they substitute simultaneously Li^+, Ta^{5+} and interstitial sites.

4. Conclusions

Temperature distributions and gradients of a temperature were determined for thermal systems with active and passive iridium afterheaters. In order to obtain high quality crystals, a thermal system should be adequately chosen. In all crystal growth runs both types of thermal systems were successively applied.

Nd, Yb:LT single crystal reveals higher optical density. It may be due to a competition between Nd and Yb in substituting LT lattice sites. Such competition is not observed for Nd, Yb:LN single crystals.

In the absorption spectrum of LT single crystals doped during growth there arises a very clear 2871 nm band due to an existence of OH^- ions in the lattice. It suggests that rare-earth ions are located in the LT lattice in other positions than Li^+ sites. In the case of doping by diffusion with Cr or Cu only weak absorption is observed near the wavelength corresponding to the OH^- line. These observations suggest that the location of active ions depends on the method of doping. In the case of doping by thermo-diffusion a decrease of intensity of OH^- absorption bands leads to the conclusion that ion dopants are introduced mainly into Li^+ sites in the LT lattice. On the other hand, doping during growth probably leads to an incorporation of active ions into Ta^{5+} sites or interstitial positions.

In the case of Pr-doped LT single crystals it seems that for low concentrations of Pr, Pr^{3+} ions substitute Ta^{5+} or interstitial sites (it is confirmed by high additional absorption after γ-irradiation), while for high concentrations they locate mainly at Li^+ positions.

For LT crystal diffusely doped with Cu and Cr transition metal ions the main factors determining thermo-diffusion process are temperature and period. Optimal conditions for obtaining good quality LT crystals doped by diffusion was a thermo-diffusion temperature equal to about 900°C and period about 20 h.

Additional absorption of LT single crystals after γ-irradiation reveal four bands with maxima 311, 394, 2871 and 4200 nm. Intensity of the first band is in the same way related to the imperfection of the crystal connected with the doping process, the second is connected with a color F-type center, the third is due to a change in OH^- ions concentration and the fourth could be connected with f–f transitions. The shallower is the first band then the better is the impurity incorporation into a crystal. We suspect that negative changes of the 2871 nm band after γ-irradiation indicate change in imperfection of the LT crystal, may be an increase of dopant ion concentration in Li^+ sites (as e.g. in the case of highly doped Pr:LT crystals). Positive change of this band may indicate an increase of dopant ion concentration in Ta^{5+} or interstitial sites (as e.g. in the case of low doped Pr:LT crystals).

Valency change of Ho and Pr ions after γ-irradiation was stated for Ho:LT and Pr:LT single crystals. It was confirmed by changes in absorption observed after annealing of the crystals in air. Probably the following recombination reactions due to Compton electrons take place: $Ho^{3+} \rightarrow Ho^{2+}$ and $Pr^{4+} \rightarrow Pr^{3+}$. In the first case we are dealing probably with the same situation as for Nd^{2+} ions observed in yttrium–aluminum garnet (YAG) crystals doped with Nd^{3+} ions. In Refs. [12,13] it was stated that Nd^{2+} ions appear in Nd:YAG crystals grown in N_2 atmosphere and are probably placed in strongly defected areas of the Nd:YAG crystal, which led to their spectral passivity. In our opinion, after analysis of changes in the absorption spectrum, the transformation $Ho^{3+} \rightarrow Ho^{2+}$ is done for about 10% of the starting Ho^{3+} concentration only.

References

[1] E.J. Lim, M.M. Fejer, R.L. Byer, Electron. Lett. 25 (1989) 174.
[2] A. Cardova-Plaza, M.J.F. Digonnet, R.L. Bayer, H.J. Shaw, IEEE J. Quantum Electron. QE-23 (1987) 262.
[3] K.S. Abedin, M. Sato, H. Ito, T. Maeda, K. Shimamura, T. Fukuda, J. Appl. Phys. 78 (2) (1995) 691.
[4] R.I. Barns, J.R. Carruthers, J. Appl. Cryst. 3 (1970) 395.
[5] H. Iwasaki, S. Miyazawa, T. Yamada, N. Uchida, N. Niizeki, Rev. Elec. Lab. 20 (1972) 129.
[6] C.D. Bandle, D.C. Miller, J. Cryst. Growth 24–25 (1974) 432.
[7] P.F. Bordui, R.G. Norwaad, C.D. Bird, J.T. Carella, J. Appl. Phys. 78 (1995) 4647.
[8] S.M. Kaczmarek, Cryst. Res. Technol. 34 (1999) 737–743.
[9] S.M. Kaczmarek, R. Jabłoński, I. Pracka, M. Świrkowicz, S. Warchoł, Cryst. Res. Technol. 34 (1999) 729–735.
[10] I. Pracka, A. Bajor, S.M. Kaczmarek, M. Świrkowicz, B. Kaczmarek, J. Kisielewski, T. Łukasiewicz, Cryst. Res. Technol. 34 (5–6) (1999) 627–634.
[11] T. Kobayashi, K. Mutto, J. Kai, A. Kawamori, J. Mag. Res. 34 (1970) 459–468.
[12] E.V. Antonov, Ch.S. Bogdasarov, N.A. Kazakov, Kristallografija 29 (1) (1984) 178–179, in Russian.
[13] N.A. Kulagin, A.E. Ovechkin, E.V. Antonov, Zhurnal Prikladnoj Spektroskopii 43 (3) (1985) 478–484, in Russian.